

Molecular modelling studies on triazole-based oxidoreductase inhibitor using 3D-QSAR

Dr. Birendra Shrivastava¹, Mr. Gajanan Bhagwat^{2*}, Dr. Rajesh Patil³, Dr. Mahaveer Singh⁴, Dr. Ashwin Porwal⁴

^{1,2,4} *Department of Pharmaceutical Chemistry, School of pharmaceutical sciences, Jaipur national University, Jaipur-302017, Rajasthan, India*

³ *Sinhgad Technical Education Society's, Smt. Kashibai Navale College of Pharmacy, Pune-Saswad Road, Kondhwa (Bk), Pune-411048, Maharashtra., India*

⁴ *Healing Hands & Herbs (R&D Center), 101, Mangalmurti Complex, Shukrawar Peth, Tilak Road, Pune 411002. Maharashtra, India*

Abstract:

The biological dataset were retrieved from four series of oxidoreductase inhibitor synthesized by Shu Zhang et al. (2017) and consisted of total 46 (forty six) oxidoreductase inhibitor. The oxidoreductase inhibitory IC₅₀ values (μM; performed against oxidoreductase from M.tuberculosis) were converted into negative logarithmic units (pIC₅₀). The compounds was further and isoniazide was used as a reference, since its crystallographic structure bound to oxidoreductase is available under PDB 5JFO. Since the inhibitors are structurally related, the training set and test set were assigned by diversity method as followed. Using this approach, the test set are spread over the whole range of activity values, and there is, at least, one test set from each range of biological activity.

Keywords: *Triazole CoMFA, CoMSIA, HQSAR, Oxidoreductase inhibitor.*

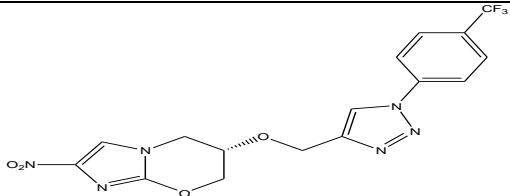
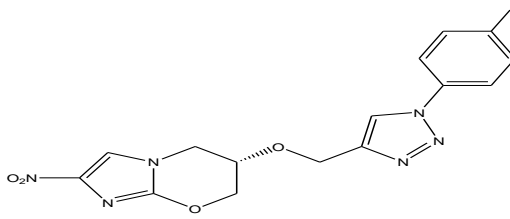
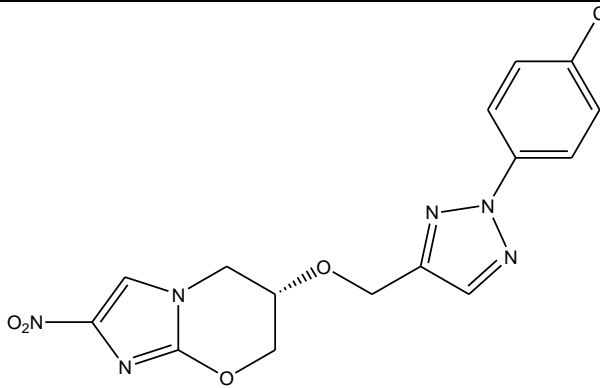
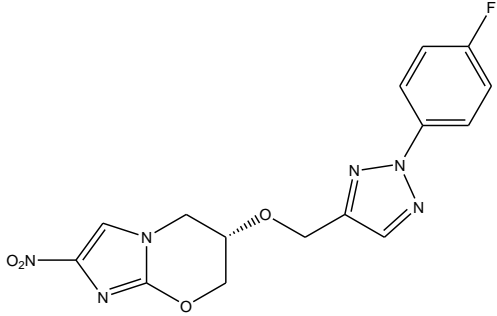
Introduction:

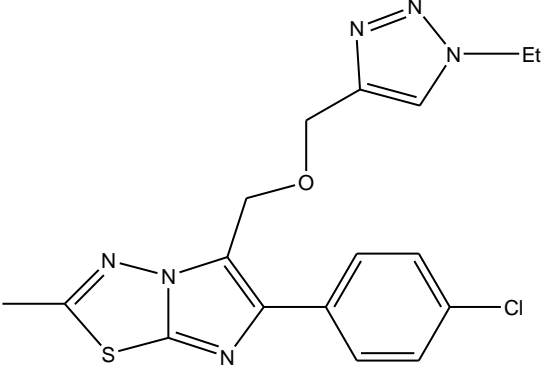
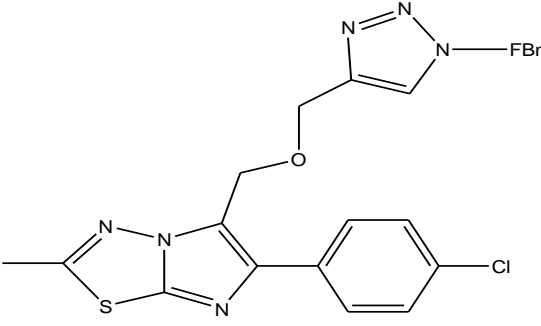
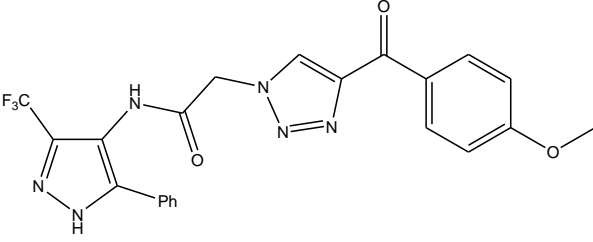
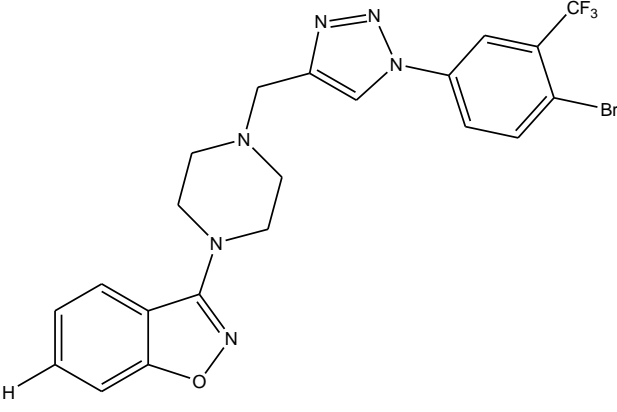
Tuberculosis (TB) remains one of the most widespread and leading deadliest diseases that result in 1.4 million deaths and 10.4 million clinical cases in the year 2015, and both are in continual increase, especially in developing countries according to the World Health Organization (WHO) 2016 report [1]. Azoles are one of the most important classes of nitrogen containing heterocycles that exhibited various biological activities such as anti-bacterial, anti-malarial, anti-fungal, anti-HIV, anti-inflammatory and anti-TB properties. In particular, triazole including 1,2,3- triazole, 1,2,4 triazole, benzotriazole, triazolopyrimidine as well as their derivatives have attracted continuous interest in the medicinal chemistry, and some drugs currently in use are based on triazoles especially 1,2,3-triazole moiety such as antiHIV agent TSAO, antibiotic Cefatrizine, anti-bacterial agent Tazobactam as well as anti-cancer agent CAI[2]. Quantitative structure-activity and relationships, often simply known as QSAR, is an analytical application that can be used to interpret the quantitative relationship between the biological activities of a particular molecule and its structure. It is considered a major method of chemical researching all over the world today and is frequently used in agricultural, biological, environmental, medicinal, and physical organic studies [3].

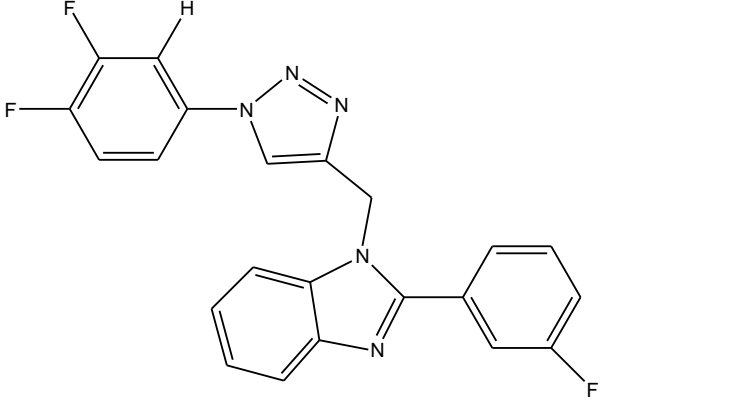
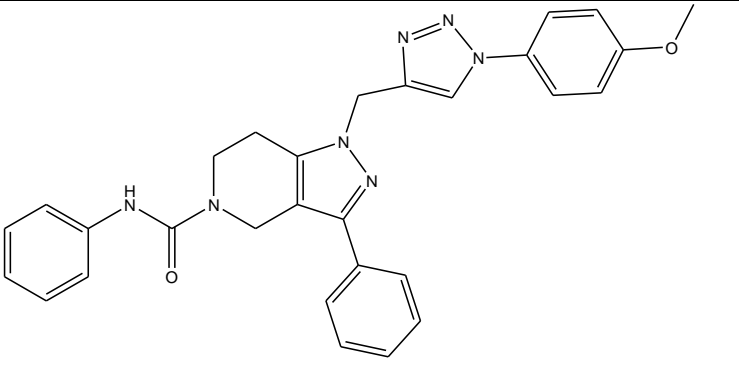
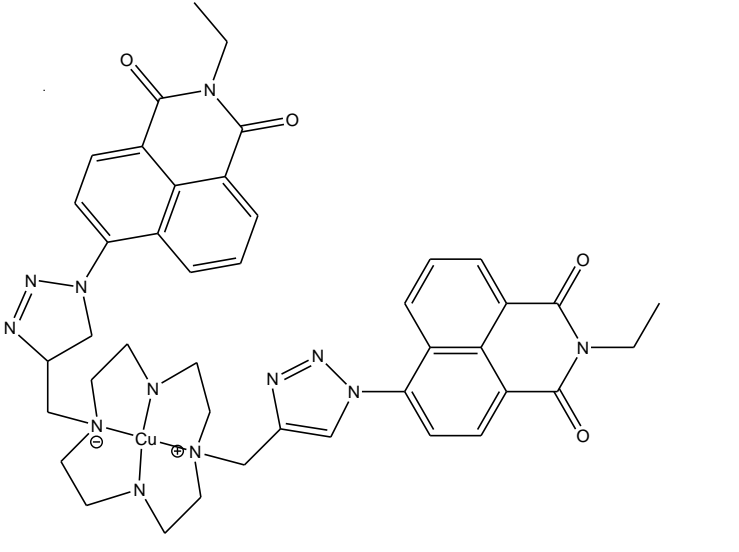
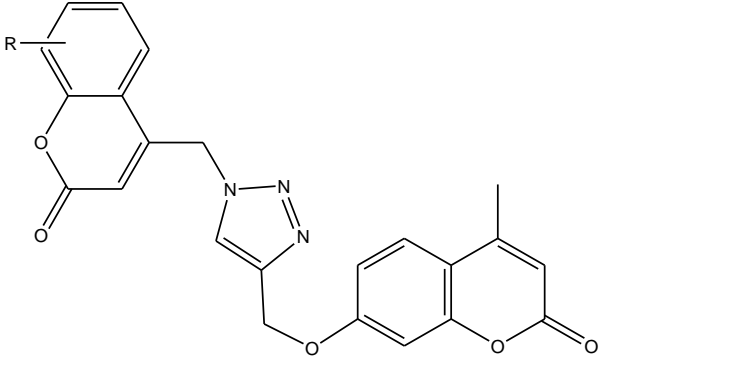
Experimental work:

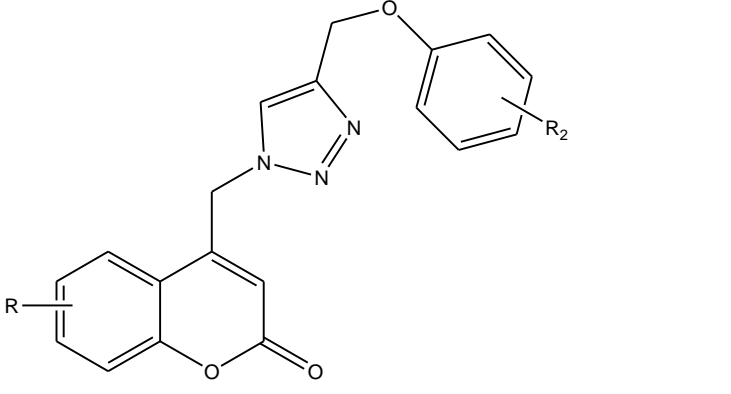
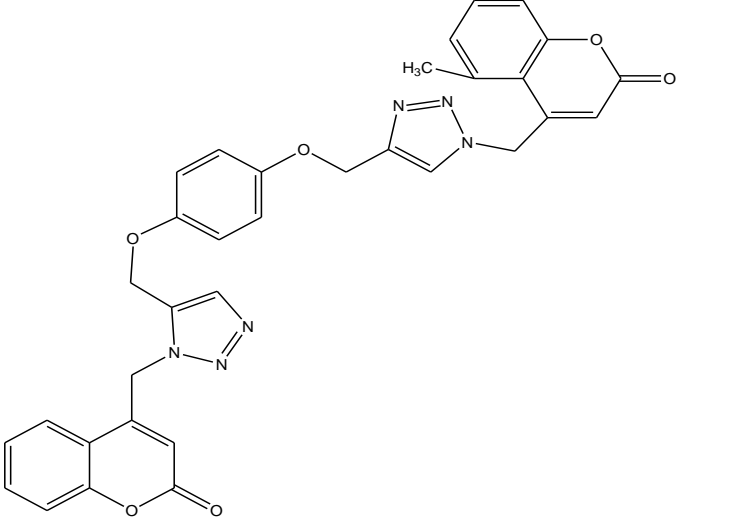
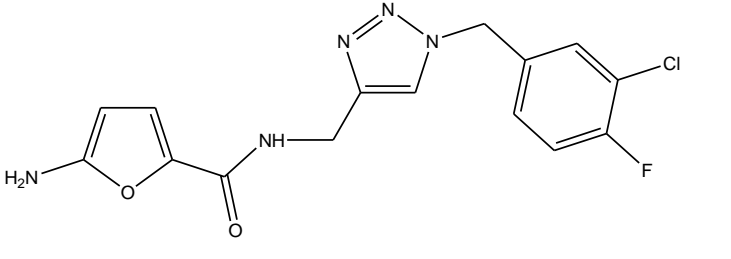
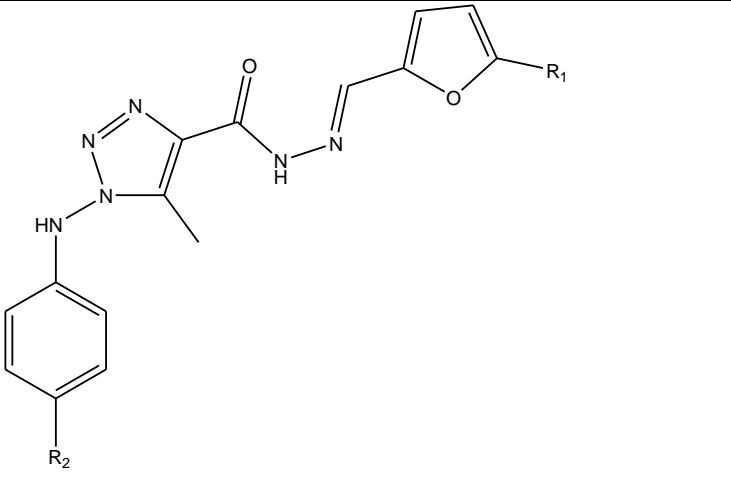
The CoMFA and CoMSIA models were developed using 37(1a, 1c, 2b-c, 3a-3b, 5a, 7a, 9, 11, 13, 15, 17a-b, 17e-f, 19, 21, 23a, 25, 27, 29a, 30b, 31b, 33c, 35d, 37b, 37c, 41, 43, 45a-c, 47b, 49, 51) as training set, and externally validated using (4, 8, 10, 12, 14, 18, 28, 38, 50) as test set.

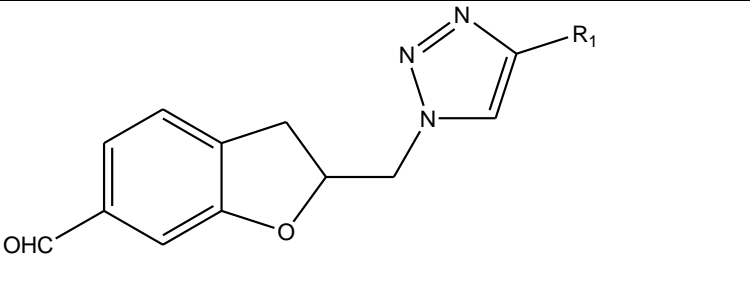
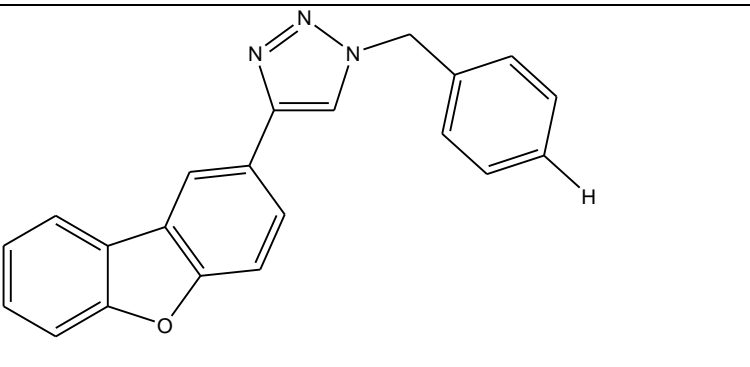
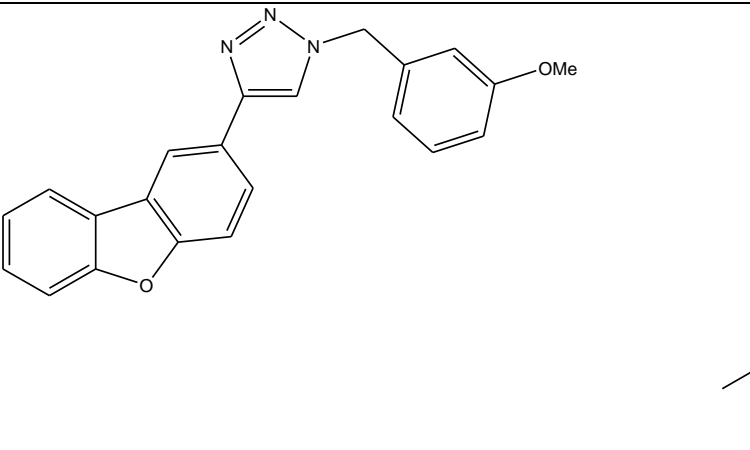
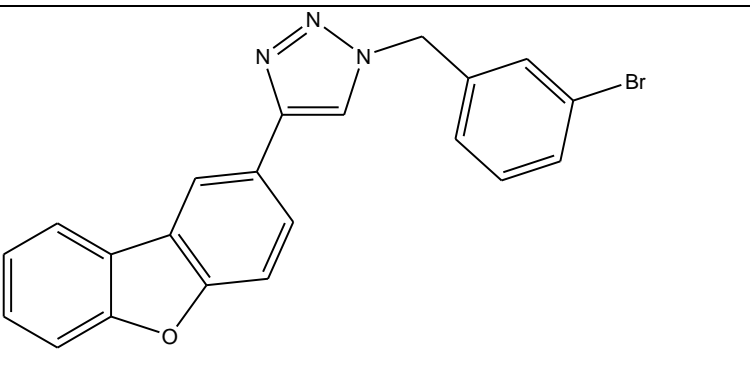
Table 1: The structures and their biological data

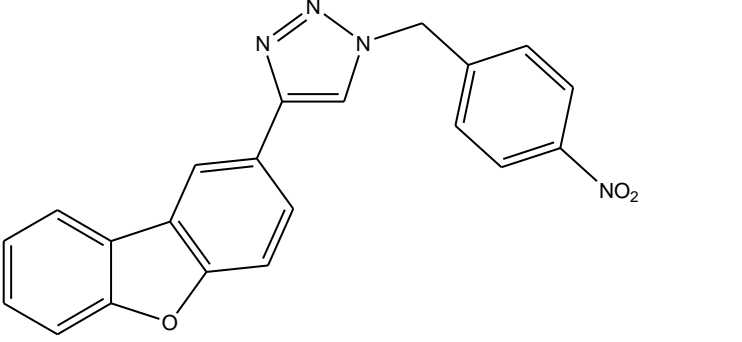
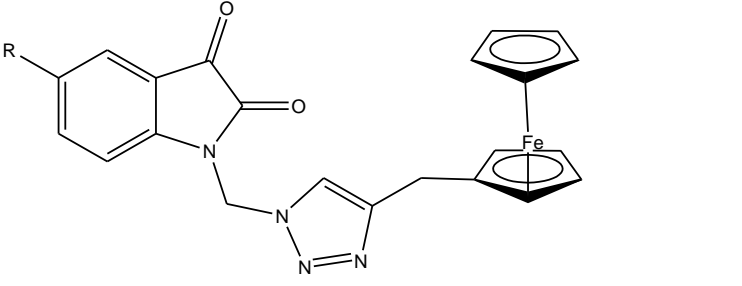
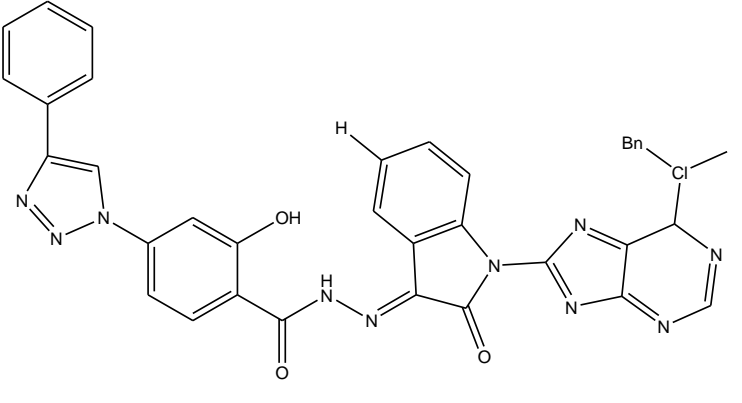
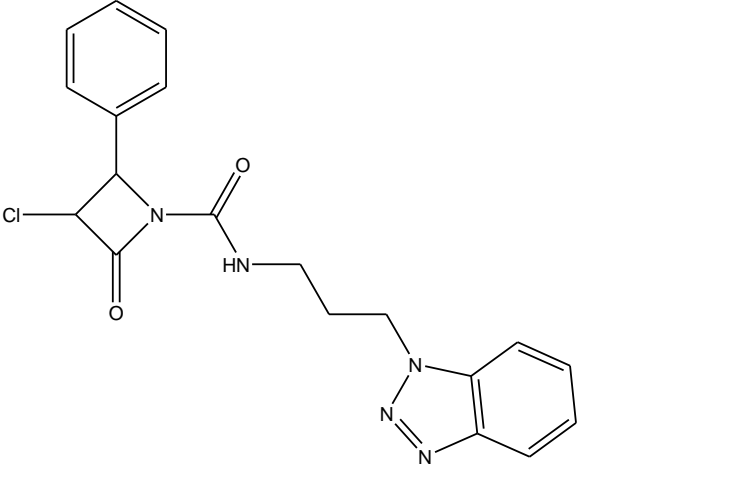
S. No.	Compound code	Compound structure	IC ₅₀ (μ M)
1	1a		112.40
2	1c		42.26
3	2b		202.16
4	2c		303.52

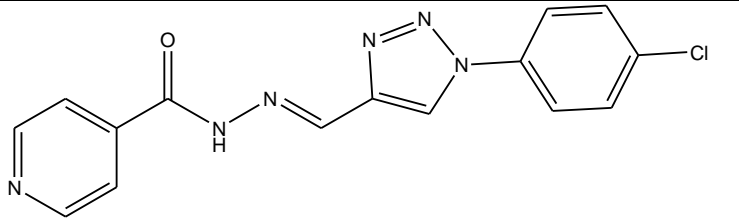
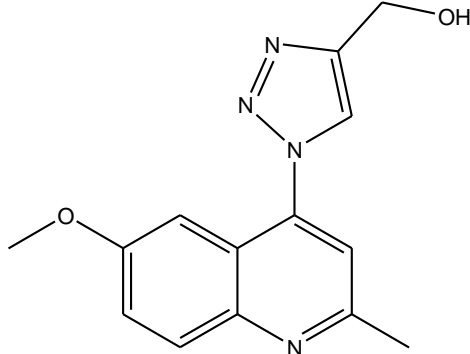
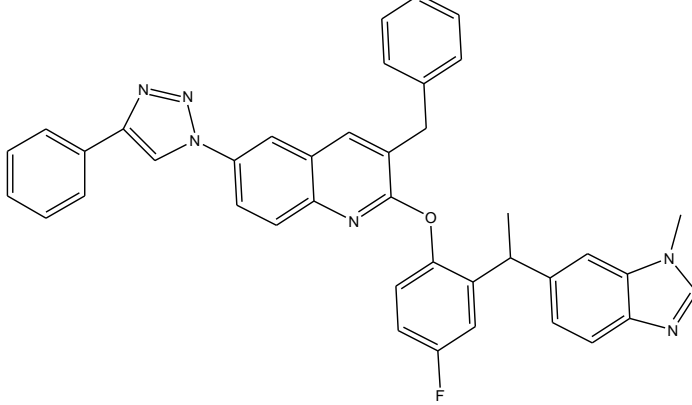
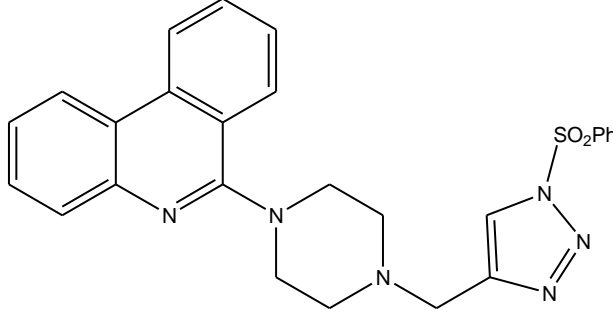
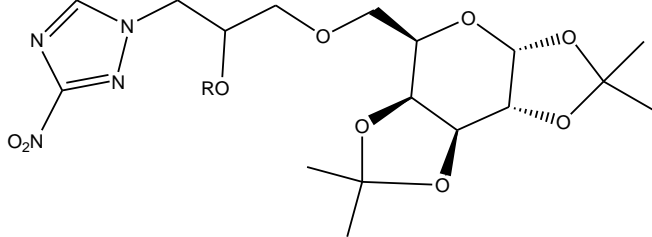
5	3a		204.44
6	3b		174.21
7	4		35.75
8	5a		16.23

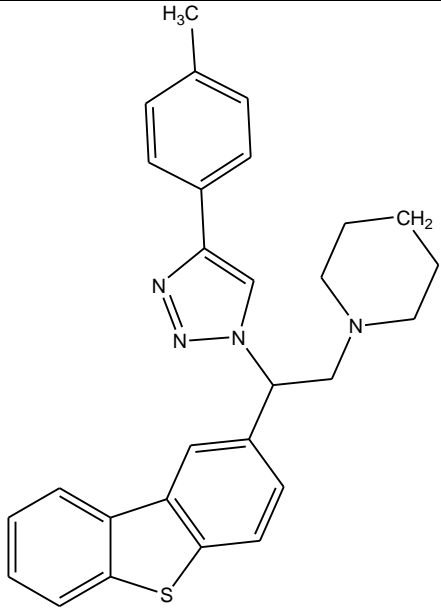
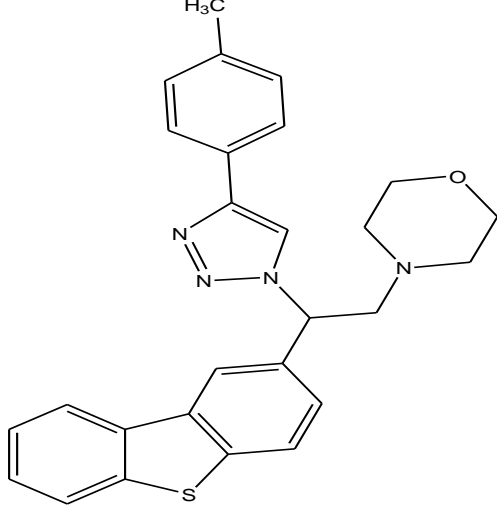
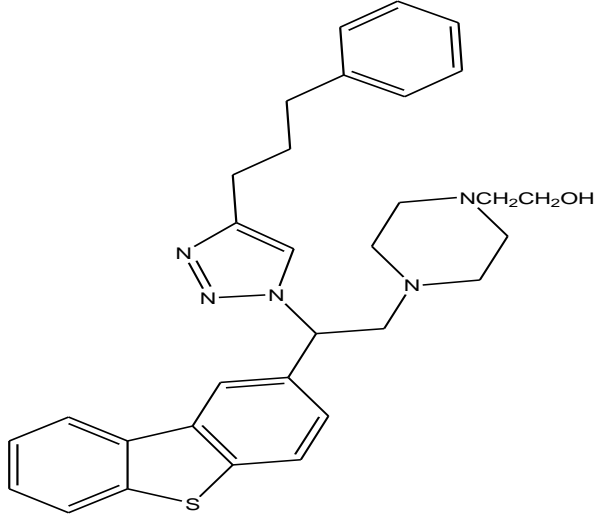
9	7a		64.52
10	8		323.91
11	9		145.40
12	10		364.41

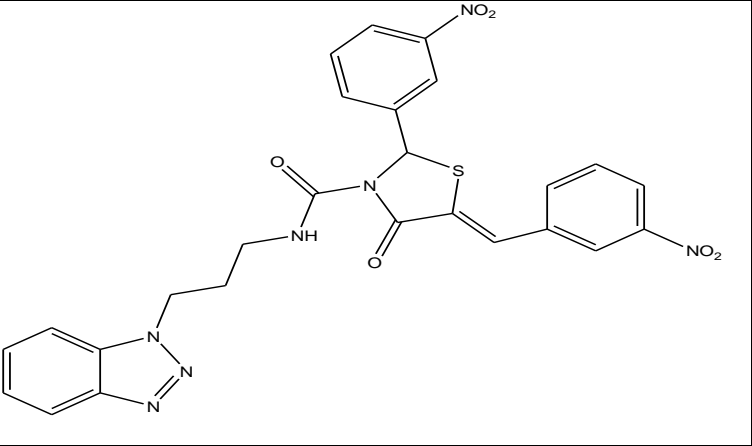
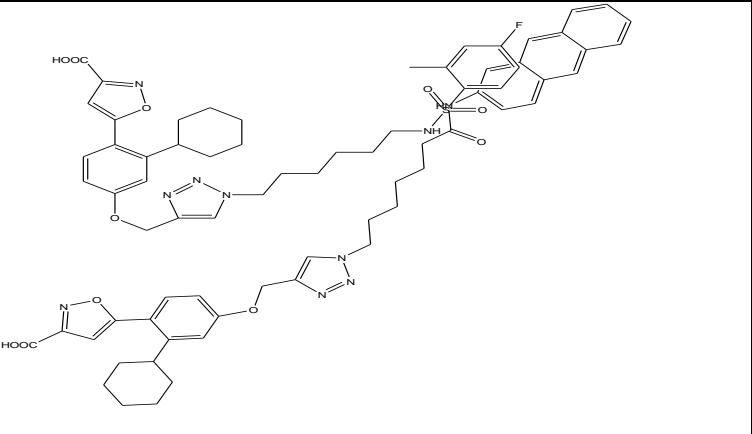
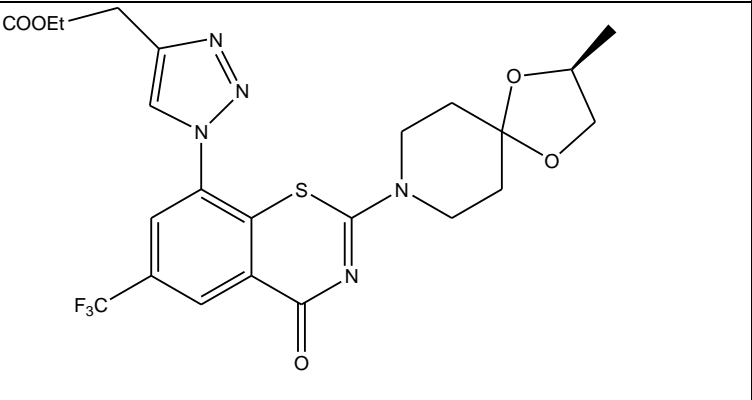
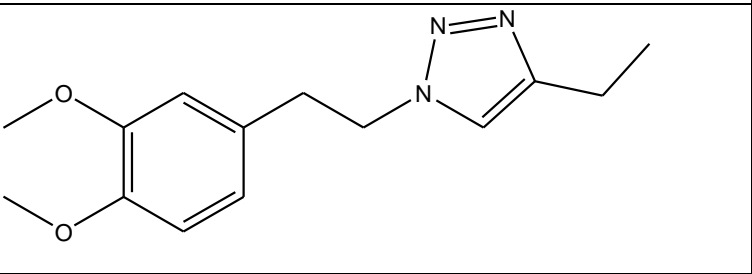
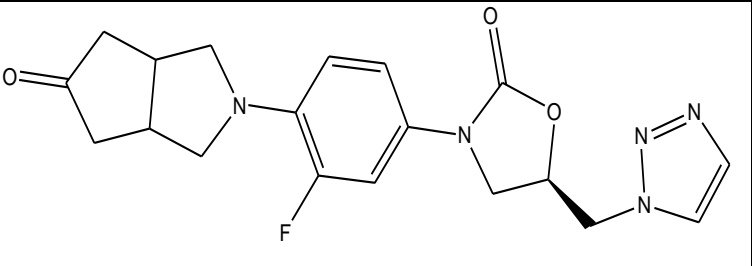
13	11		181.70
14	12		142.81
15	13		193.55
16	14		99.16

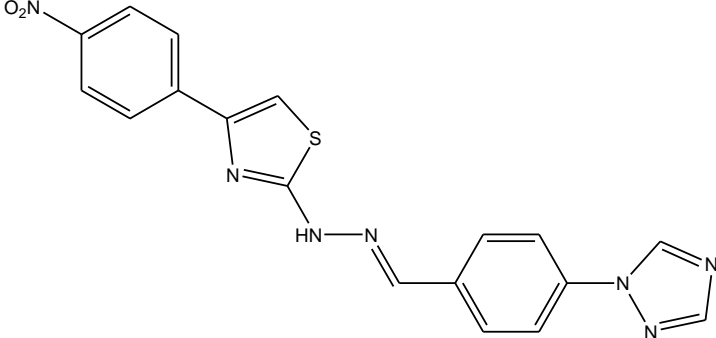
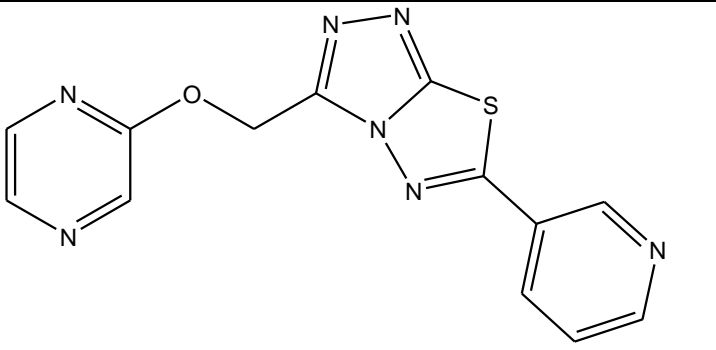
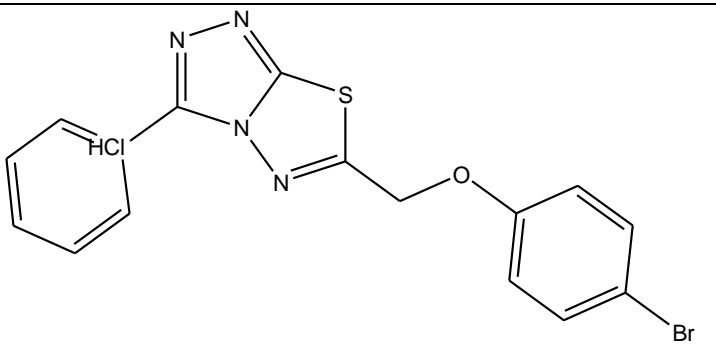
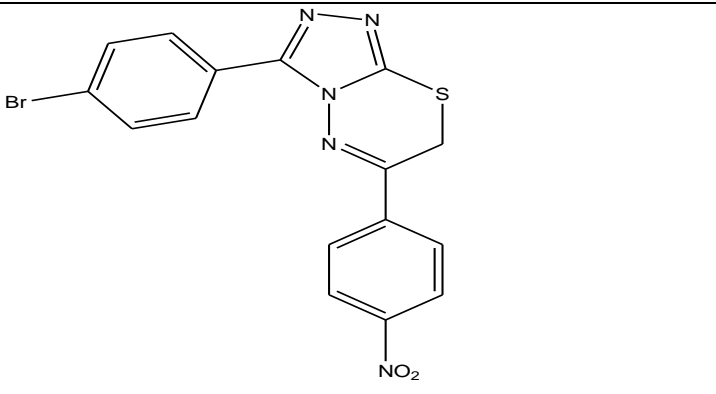
17	15		123.32
18	17a		55.43
19	17b		226.32
20	17e		175.72

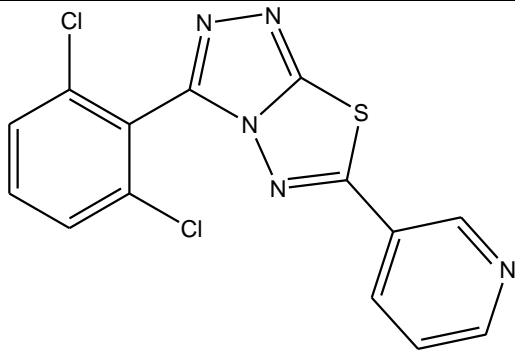
21	17f		46.39
22	18		6.50
23	19		10.23
24	21		11.29

25	23a		8.48
26	25		11.22
27	27		6.97
28	28		5.55
29	29a		12.75

30	30b		15.09
31	31b		5.58
32	33c		26.38

33	35d		7.12
34	37b		16.17
35	37c		8.05
36	38		28.02
37	41		18.33

42	47b		9.12
43	48		53.34
44	49		44.8
45	50		11.85

46	51		11.12
----	----	---	-------

Structural Alignment:

The molecular modelling studies were performed using SYBYL X2.0 software (Tripos) running on a core-2 duo Intel processor workstation [4]. The molecules to be analysed were aligned on an appropriate template, which is considered to be common substructure.

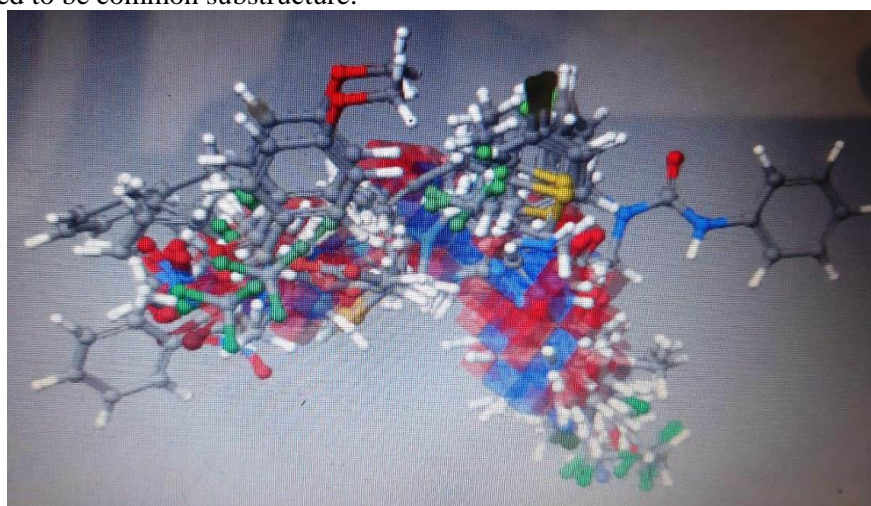


Figure 1: Alignment of all selected molecules

CoMFA:

The aligned sets of molecules were positioned inside four grids boxes with grid spacing values of 1.5, 2.0, 2.5 and 3.0 Å in all Cartesian directions and CoMFA fields were calculated using the QSAR modules of SYBYL. The steric (vdW interaction) and electrostatic (Coulombic values with a 1/r distance-dependent dielectric function) fields were calculated at each intersection on the regularly spaced grid [5]. In order to reduce noise and improved efficiency, column filtering (minimum sigma) was set to 2.0 kcal mol⁻¹, excluding from the analysis those column (lattice points) whose energy variance is less than 2.0 kcal mol⁻¹.

CoMSIA:

In CoMSIA, the steric indices are related to the third power of the atomic radii, the electrostatic descriptors are derived from atomic partial charges, the hydrophobic fields are derived from atom-based parameters, and the hydrogen bond donor and acceptor indices are obtained from a rule-based method derived from experimental values [6-8]. A Gaussian function is used to evaluate the mutual distance between the probe atom and each molecule atom. Because of the different shape of the Gaussian function, the similarity indices (A) can be calculated at all grid points of the molecular surface according to equation (1).

$$A_{F,k}^q(j) = \sum W_{\text{probe},k} W_{ik} e^{-\alpha r_{ik}^2}$$

HQSAR:

The fragment distinct are atoms (A), bonds (B), connections (C), hydrogen atom (H), chirality (Ch), and donor (D). Initially, various models were developed by using the default fragment size of 4-7 and different component, then based on the different fragment distinction determined by the first step, the models were developed using different sizes [9, 10]. The models with better results were applied to different fragment size and component number (Jae et al., 2008).

Result and Discussion:

The CoMFA models MMFF94 were generated from training set of 37 molecules with pIC₅₀ value ranging from 3.4661 to 5.2749 using leave-one-out PLS analysis with an optimized component of 1 to give a good cross-validated correlation coefficient q^2 of 0.787, which suggest that the model should be reasonable tool for predicting the IC₅₀ values. The results of CoMSIA analysis with different combination on different charge are summarized. Among the combination models, steric, electrostatic, acceptor, donor and hydrophobic fields played an essential roles for the present series of compounds [11-13]. Removal of any descriptors results in significant reduction in r^2 , q^2 and r^2_{pred} , which implies that all descriptors all descriptors are crucial and the steric, electrostatic, hydrophobic, donor and acceptor functional groups were of extreme significance for the inhibitory activity. In conclusion, the combination of steric, electrostatic, hydrophobic, donor and acceptor was selected as the best model.

Table 2: CoMFA on different charge

Sno	Model	q^2	r^2	SE	NC
1	Model 1 Gastegier	0.775	0.816	0.265	1
2	Model 2 G-H	0.786	0.819	0.262	1
3	Model 3 Delre	0.771	0.814	0.266	1
4	Model 4 Pullman	0.780	0.814	0.266	1
5	Model 5 Formal Charge	0.779	0.812	0.266	1
6	Model 6 MMFF94	0.787	0.819	0.262	1

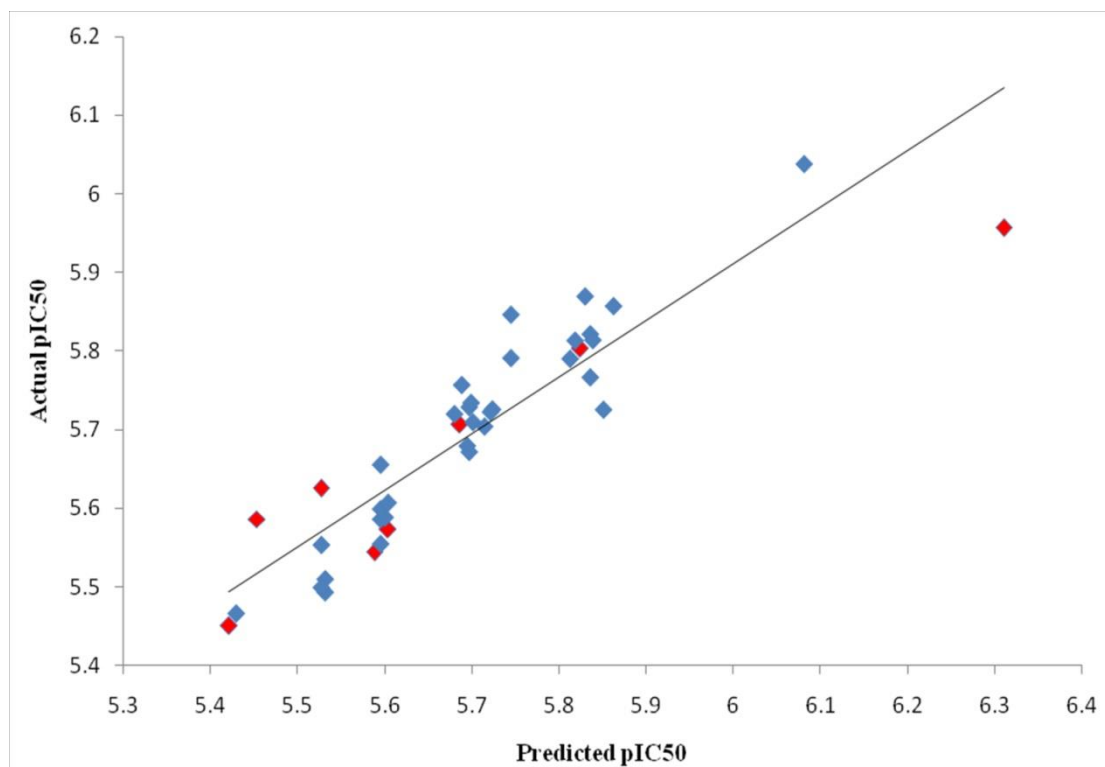


Figure 1: Graph of actual versus predicted pIC₅₀ values of the training set and the test set using the CoMFA model.

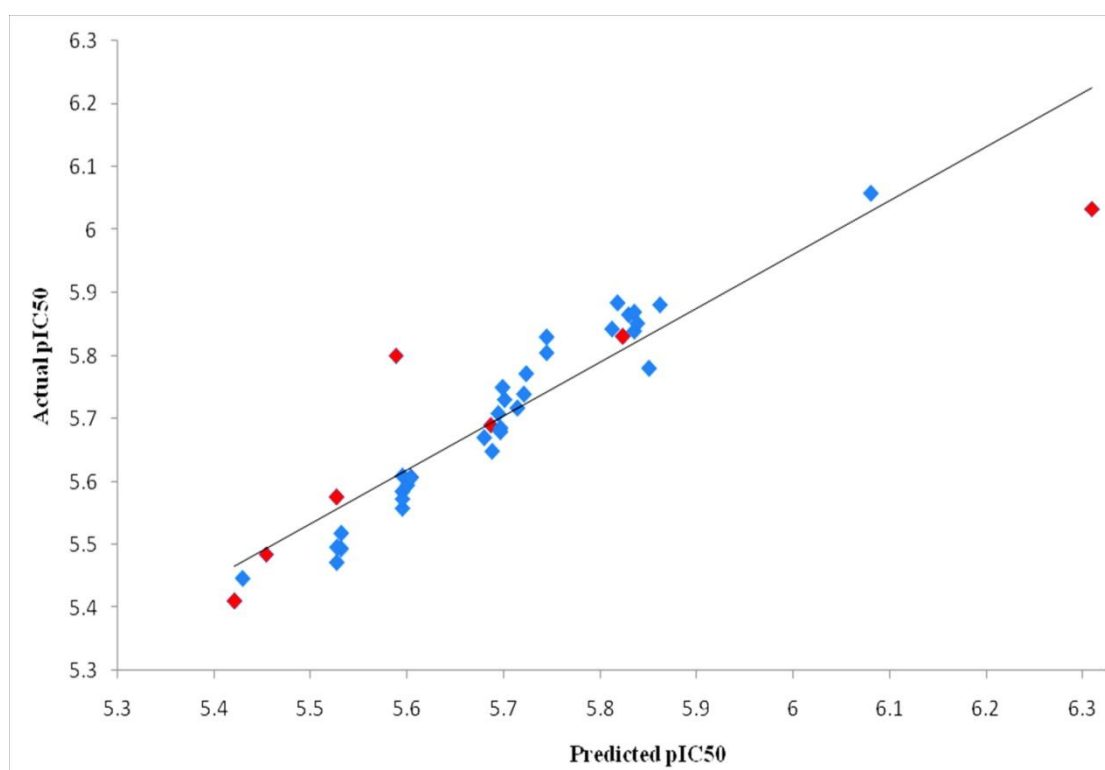


Figure 2: Graph of actual versus predicted pIC₅₀ values of the training set and the test set using the CoMSIA model.

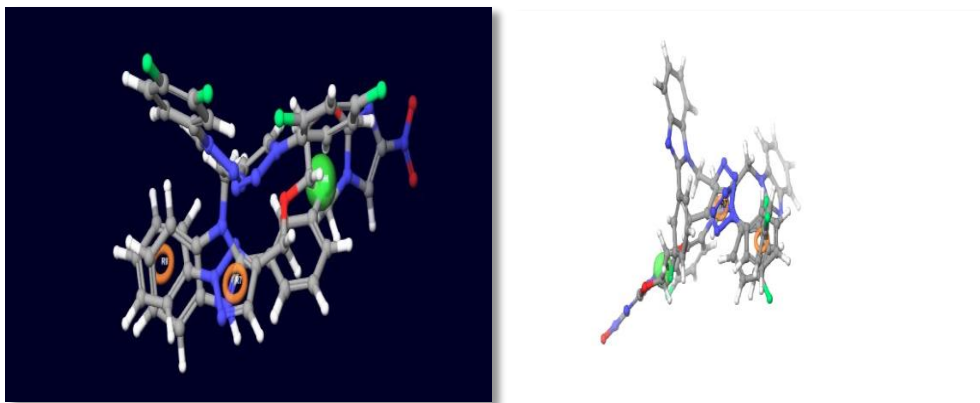


Figure 3: Contour map of Compound 26 and 13.

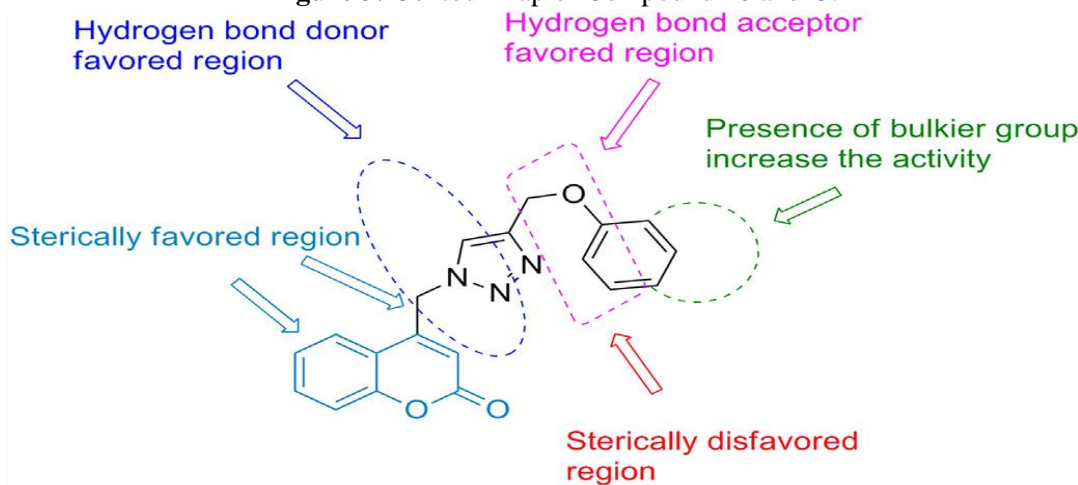


Figure 4: 3D-QSAR of compound for designing.

CoMSIA contour Maps:

The best combination models for CoMSIA were steric, electrostatic, hydrophobic, donor and acceptor fields and the contour showed in Figure 5.4. The steric fields is characterised by green and yellow contour, in which yellow contour is unfavourable for the introduction of bulky group, while the green contour is favourable for the introduction of the bulky groups.

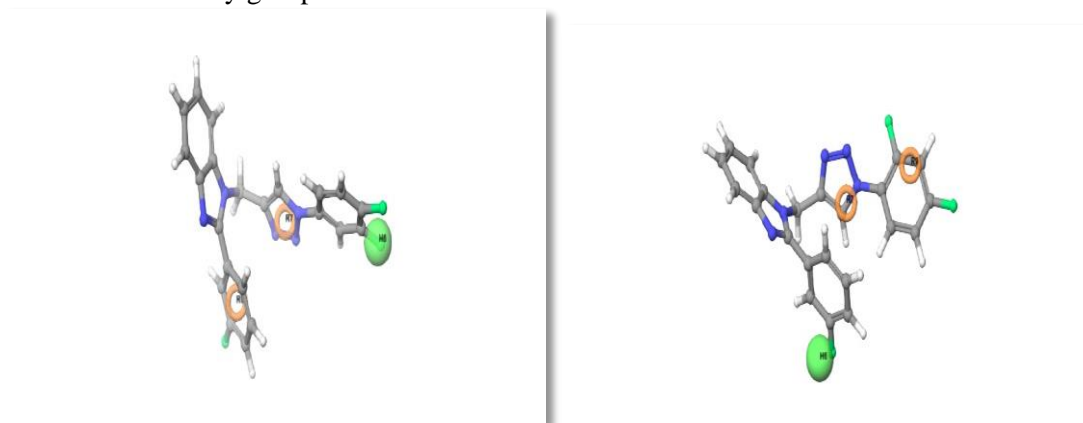


Figure 5: Contour map of Compound 36 and 13 Steric

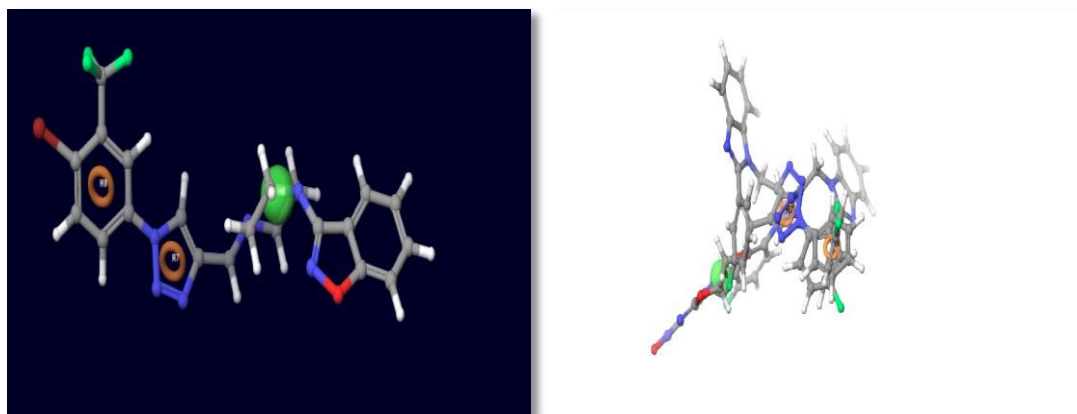


Figure 6: Contour map of Compound 13 and 36 electrostatic

HQSAR Results:

HQSAR investigations require selecting values for the parameters that specify the hologram length, as well as the size and type of fragments to be encoded. The generation of the molecular fragments was performed using the following fragments distinction parameters: atoms (A), bonds (B), connections (C), hydrogen (H) atoms, chirality (Ch) and donor/acceptor (DA) atoms. For the training set, a default fragment size (4-7) was employed to obtain relevant statistical indexes with different combinations of fragment distinction parameters A/B, A/B/H, A/B/C, A/B/Ch, A/B/C/H, A/B/DA, A/B/C/DA, A/B/C/Ch, A/B/H/DA, A/B/H/Ch, A/B/Ch/DA, A/B/C/H/DA, A/C/H/DA, A/C/H/Ch/DA. To improve these statistical indexes, we investigated the influence of fragment size (1a, 1c, 2b-c, 3a-3b, 5a, 7a, 9, 11, 13, 15, 17a-b, 17e-f, 19, 21, 23a, 25, 27, 29a, 30b, 31b, 33c, 35d, 37b, 37c, 41, 43, 45a-c, 47b, 49, 51) on the fragment distinction parameters of those models having the highest statistical indexes.

Table 3: The determination of statistical parameters for the model of the series based on different fragment size fragment distinct A/B/C.

Sno	Name	q ²	r ²	q ² SE	r ² SE	Ensemble	Best length	NC
1	2-5	0.800	0.907	0.276	0.204	0.903	97	6
2	3-6	0.800	0.921	0.277	0.188	0.917	307	6
3	4-7	0.800	0.943	0.250	0.160	0.933	257	6
4	5-8	0.785	0.953	0.286	0.144	0.945	307	6
5	6-9	0.786	0.952	0.290	0.146	0.946	151	6
6	7-10	0.781	0.957	0.293	0.138	0.951	257	6
7	8-11	0.779	0.959	0.299	0.135	0.956	307	6
8	2-6	0.801	0.920	0.276	0.189	0.917	151	6
9	3-7	0.799	0.951	0.277	0.148	0.933	257	6
10	4-8	0.787	0.951	0.289	0.148	0.942	151	6
11	5-9	0.791	0.949	0.291	0.151	0.944	353	6
12	6-10	0.785	0.954	0.246	0.143	0.947	257	6

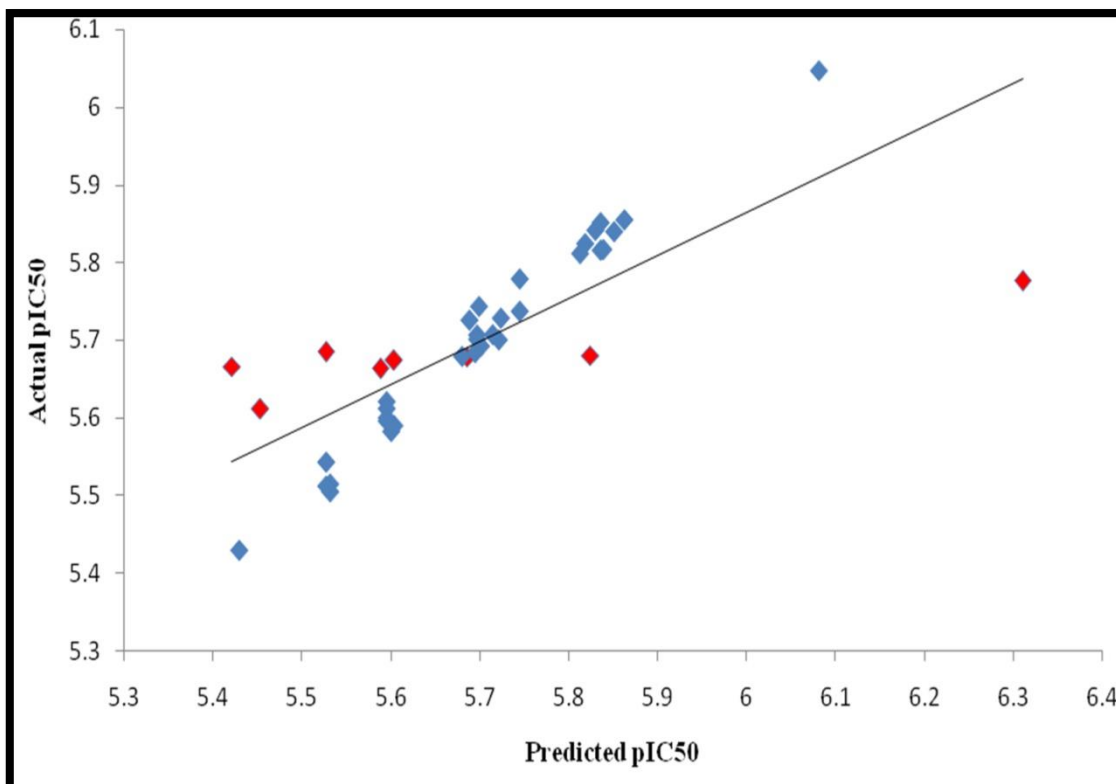


Figure 7: Graph of actual versus predicted pIC₅₀ values of the training set and the test set molecules of Model A/B/C at 2-6 fragment size using the HQSAR.

Conclusion:

The present work describes successfully applied QSAR study to characterize set of triazole derivatives and to identify essential structural requirements in 3D chemical space for the modulation and optimization of oxidoreductase inhibitor activity. The CoMFA, CoMSIA and HQSAR models showed meaningful statistical significance results in internal validation (q^2), external validation (r^2) and predicted r^2 for triazole and 1,2,3-triazole and 1,2,4-triazole derivatives. The models generated through three layered QSAR approach exhibited reliable, ease correlative and predictive abilities. The explored CoMFA and CoMSIA models provided information about favorable and unfavorable region while HQSAR provides information about positive, negative and intermediate contribution of sub-structural fingerprint requirements for imparting the biological activity. The CoMFA, CoMSIA and HQSAR contour maps revealed sufficient information to understand the structure-activity relationship (SAR) and to recognize structural features influencing inhibitory activity.

References:

1. Christian P & Stewart C. Maternal micronutrient deficiency, fetal development, and the risk of chronic disease. *The Journal of nutrition*.140, 2010, 437–45.
2. Cohen P &Goedert M. GSK3 inhibitors: development and therapeutic potential. *Nature Review of Drug Discovery*. 3, 2004, 479–48.
3. Cooke D &Plotnick L. Type 1 diabetes mellitus in pediatrics". *Paediatric Review*. 11, 2008 374–84.
4. Zhang S, Xu Z, Gao C, Ren QC, Chang L, Lv ZS, Feng LS. Triazole derivatives and their anti-tubercular activity. *European journal of medicinal chemistry*. 2017 Sep 29;138:501-13.
5. Desai NC, Trivedi AR, Khedkar VM. Preparation, biological evaluation and molecular docking study of imidazolyl dihydropyrimidines as potential Mycobacterium tuberculosis dihydrofolate reductase inhibitors. *Bioorganic & medicinal chemistry letters*. 2016 Aug 15;26(16):4030-5.
6. Sengupta S, Roy D, Bandyopadhyay S. Structural insight into Mycobacterium tuberculosis maltosyl transferase inhibitors: pharmacophore-based virtual screening, docking, and molecular dynamics simulations. *Journal of Biomolecular Structure and Dynamics*. 2015 Dec 2;33(12):2655-66.

7. Martins F, Santos S, Ventura C, Elvas-Leitão R, Santos L, Vitorino S, Reis M, Miranda V, Correia HF, Aires-de-Sousa J, Kovalishyn V. Design, synthesis and biological evaluation of novel isoniazid derivatives with potent antitubercular activity. *European journal of medicinal chemistry*. 2014 Jun 23;81:119-38.
8. Koch O, Jäger T, Heller K, Khandavalli PC, Pretzel J, Becker K, Flohe L, Selzer PM. Identification of *M. tuberculosis* thioredoxin reductase inhibitors based on high-throughput docking using constraints. *Journal of Medicinal Chemistry*. 2013 Jun 27;56(12):4849-59.
9. Naqvi A, Malasoni R, Srivastava A, Pandey RR, Dwivedi AK. Design, synthesis and molecular docking of substituted 3-hydrazinyl-3-oxo-propanamides as anti-tubercular agents. *Bioorganic & medicinal chemistry letters*. 2014 Nov 15;24(22):5181-4.
10. Al-Tamimi AM, Mary YS, Miniyar PB, Al-Wahaibi LH, El-Emam AA, Armaković S, Armaković SJ. Synthesis, spectroscopic analyses, chemical reactivity and molecular docking study and anti-tubercular activity of pyrazine and condensed oxadiazole derivatives. *Journal of Molecular Structure*. 2018 Jul 15;1164:459-69.
11. Kumar M, Vijayakrishnan R, Rao GS. In silico structure-based design of a novel class of potent and selective small peptide inhibitor of *Mycobacterium tuberculosis* Dihydrofolate reductase, a potential target for anti-TB drug discovery. *Molecular diversity*. 2010 Aug 1;14(3):595-604.
12. El-Azab AS, Mary YS, Abdel-Aziz AA, Miniyar PB, Armaković S, Armaković SJ. Synthesis, spectroscopic analyses (FT-IR and NMR), vibrational study, chemical reactivity and molecular docking study and anti-tubercular activity of condensed oxadiazole and pyrazine derivatives. *Journal of Molecular Structure*. 2018 Mar 15;1156:657-74.
13. Pulaganti M, Banaganapalli B, Mulakayala C, Chitta SK, Anuradha CM. Molecular modeling and docking studies of O-succinylbenzoate synthase of *M. tuberculosis*—a potential target for antituberculosis drug design. *Applied biochemistry and biotechnology*. 2014 Feb 1;172(3):1407-32.